PHYSICAL REVIEW A VOLUME 26, NUMBER 5 NOVEMBER 1982

Elastic and rotational excitation of the nitrogen molecule by intermediate-energy electrons

P. K. Bhattacharyya
Department of Physics, Calcutta University, 92 Acharyya Prafulla Chandra Road, Calcutta 700009, India

K. K. Goswami
Department of Physics, Rishi Bankim Chandra College, Naihati, 24-Parganas, West Bengal, India

(Received 20 May 1981; revised manuscript received 9 December 1981)

An adiabatic approximation in which the eikonal elastic amplitude for fixed molecular orientation is used as input is employed for the calculation of pure elastic scattering ($J=0\rightarrow J'=0$ and $J=1\rightarrow J'=1$), pure rotational excitation ($J=0\rightarrow J'=2$ and $J=1\rightarrow J'=3$), and orientationally averaged elastic cross sections of the nitrogen molecule in its ground electronic and vibrational states using electrons as incident particles. Both differential and integral cross sections are computed at electron energies 20—200 eV. Total momentum-transfer cross sections are also calculated. The effect of target polarization is considered in the effective electron-molecule potential. The effect of electron exchange is not taken into account. Results obtained are compared with those of other theoretical and experimental workers. The qualitative features of the rotational-excitation cross sections are found to resemble those of the hydrogen molecule. Small-angle experimental elastic cross sections are well reproduced.

I. INTRODUCTION

The study of the elastic and different inelastic processes involved in the scattering of energetic electrons from molecular nitrogen is very important in the field of atmospheric physics. From a theorist's point of view the nitrogen molecule, being moderately aspherical and not containing too many electrons, is an interesting test target for our understanding of the electron-molecule scattering problem. At low energy, which is roughly defined as impact energies less than the ionization potential, e-N_2 scattering has been studied more or less extensively using different approximations. Early investigators studied the low-energy elastic scattering of electrons from molecular nitrogen using the fixed-nuclei theory[1,2] and the rotational excitation of this molecule by employing the first Born,[3] adiabatic,[4] and distorted-wave[5–7] approximations. More recent investigators used the close-coupling,[8–11] R matrix,[12] low-l spoiling,[13] hybrid,[14] and multiple scattering[15–17] methods. A number of excellent articles[18–21] which review in detail the scattering of slow electrons by molecules, including nitrogen, have already been published. At high energy, which is defined as impact energies ten or more times the ionization potential, the e-N_2 scattering problem can be treated using high-energy approximations such as the polarized Born[22,23] and eikonal[24] approximations. At still higher energies the Born approximation becomes applicable.

It is the intermediate-energy region, roughly characterized as impact energies from the ionization potential to ten times the ionization potential, where the computation of electron-molecule scattering cross sections is most difficult.[25,26] This energy region is usually studied[26] employing either the high-energy techniques such as the polarized Born approximation[23] or the low-energy techniques such as the converged close-coupling approximation.[26] For the nitrogen molecule an extensive and systematic study has recently been done by Truhlar and co-workers[26–38] using the effective potential approach.[25] They have improved, step by step, the effective electron-nitrogen-molecule potential in respect of contributions from static,[30,35] exchange[30–32,34] and polarization interactions,[29–31] and they compared the effects of different local exchange potentials[33,35,37] and different polarization potentials[30] on the cross sections. The rotational motion was treated using either the bodyframe[35–37] or the laboratory-frame[26–34] versions[8,39] of the close-coupling approximation, and the vibrational motion, when allowed, was treated by the vibrational sudden approximation[32,34] or by the close-coupling method.[27] As a result of this investigation quite accurate and converged elastic and inelastic cross sections[32,34] for e-N_2 scattering are now available up to an impact energy of 50 eV. The intermediate-energy e-N_2 scattering has also been studied using the continuum-multiple-scattering method[40] by Dill and Dehmer[15] and Siegel *et al.*,[16,17] the independent-particle model by Sawada *et al.*[41] and Wedde and Strand,[42] and the two-potential approach by Choi *et al.*[43]

In recent years the Glauber-type[44] eikonal scattering amplitude has received considerable attention in the field of electron-atom scattering.[45–48] This approximation, which is expected to be most valid at high energy and at small scattering angles, is found[49] to be applicable even at intermediate energies and at intermediate scattering angles. Moreover, it obeys the important constraint of unitarity. Only a few attempts[24,50–57] have been made to investigate the electron-molecule scattering problem using the Glauber approximation. At intermediate energies the vibrational excitation of the hydrogen molecule was studied by Chang *et al.*,[50] while the elastic scattering and rotational excitation were first studied by Bhattacharyya and Ghosh,[51,52] and Bhattacharyya *et al.*[53] The rotational excitation of a strongly polar molecule (CsCl) was considered by Ashihara *et al.*[54] at low energy. Subsequently, Gianturco and coworkers[55–57] computed rotational-excitation cross sections of a few molecules, including nitrogen, in which they have considered only the asymptotic part of the static[55,56] and static plus polarization[57] potentials.

In the present paper we have used[52,53] the Glauber-type eikonal amplitude for a fixed molecular orientation in the framework of the adiabatic approximation to investigate the problem of elastic scattering and rotational excitation of the molecular nitrogen initiated by intermediate-energy (20–200-eV) electrons. The eikonal amplitude and the different scattering cross sections obtained as a result are expressed in terms of a highly convergent series involving a product of Bessel functions of increasing order. The convergence of higher-order terms is related to the fact that these terms contribute only to higher elastic or rotational-excitation states. For the effective electron-molecule potential, we have considered the polarization potential in addition to the static potential. Effects of electron exchange are neglected. The present study is the outcome of the following consideration: it is well known that the Born approximation is inaccurate at intermediate energies. On the other hand, a converged close-coupling calculation is almost prohibitive for all but a few simple molecules.[58] Thus, one should try a simple theory, such as the present one, and find out how well it can describe the scattering phenomena. We have shown earlier[53] that the Glauber-type eikonal approximation can explain successfully the scattering of intermediate-energy electrons from the almost "atomlike" hydrogen molecule. The extension of this approximation to a more complex target is needed to learn about its applicability to complex targets in general. In this respect nitrogen is an ideal test target. This is because for nitrogen accurate close-coupling cross sections[32,34] at the lower part of the intermediate-energy region as well as reliable experimental data[59–64] are available, and a comparison of the predictions of the present approximation with them might provide useful information.

The presentation is organized as follows. A brief outline of the theory is given in Sec. II. The effective electron-nitrogen-molecule potential is discussed in Sec. III. Results of the present calculation and their comparison with those of other theoretical and experimental workers are presented in Sec. IV. Finally, concluding remarks are given in Sec. V.

II. THEORY

The method used for the present calculations has been presented elsewhere[52,53] in detail. Here we give[65] a brief outline of it. We consider the homonuclear diatomic molecule as a rigid rotor having an internuclear separation equal to R. In the adiabatic approximation[19] the differential scattering cross sections $I(J\rightarrow J',\theta)$ for the excitation process $(J\rightarrow J')$ and the average elastic differential scattering cross section $\langle I(\theta)\rangle$ are, respectively, given by

$$I(J\rightarrow J',\theta) = \frac{1}{2J+1}\sum_{M,M'} \left| Y^{*}_{J'M'}(\hat{R})f(\theta,\hat{R})Y_{JM}(\hat{R})d\hat{R}\right|^{2} \tag{1}$$

and

$$\langle I(\theta)\rangle=\frac{1}{4\pi}\int \left|f(\theta,\hat{R})\right|^2 d\hat{R}\ , \tag{2}$$

where the spherical harmonic Y_{JM}'s are the target wave functions, θ is the scattering angle, and $f(\theta,\hat{R})$ is the scattering amplitude for a fixed orientation of $\vec{R}$ ($\hat{R}$ is the unit vector along $\vec{R}$). As Eq. (1) suggests, the amplitude $f(\theta,\hat{R})$ is alone sufficient to yield pure elastic scattering and pure rotational-excitation cross sections.

To obtain the eikonal scattering amplitude we expand the effective interaction potential $V(\vec{r},\hat{R})$ in terms of the even-order Legendre polynomials

$$V(\vec{r},\hat{R})=\sum_{\nu=0} V^{\nu}(r)P_{\nu}(\vec{r}\cdot\hat{R})\ , \tag{3}$$

where $\vec{r}$ denotes the position vector of the scattered electron measured from the center of mass of the two nuclei of the target. If we consider the first two nonvanishing terms of the above expansion then a convenient form of the eikonal amplitude for the scattered electron is obtained[52]

$$f(\theta,\hat{R})=-ik_i\sum_{n=0} i^n\lambda_n f_{2n,n}(\theta,\theta_m)\cos 2n\phi_m\ , \tag{4}$$

with

$$f_{2n,n}(\theta,\theta_m)=\begin{cases}\int_0^\infty J_0(qb)[e^{-i\chi(b,\theta_m)}J_0(\gamma)-1]b\,db & \text{for } n=0,\\ \int_0^\infty e^{-i\chi(b,\theta_m)}J_{2n}(qb)J_n(\gamma)b\,db & \text{for } n\neq 0,\end{cases}$$

$$\chi(b,\theta_m)=\frac{2}{v_i}\int_0^\infty V^0(r)dz+\frac{1}{v_i}(1-\tfrac{3}{2}\sin^2\theta_m)\int_0^\infty V^2(r)\frac{2z^2-b^2}{r^2}dz\ ,$$

$$\gamma(b,\theta_m)=\tfrac{3}{2}\frac{\sin^2\theta_m}{v_i}\int_0^\infty V^2(r)\frac{b^2}{r^2}dz\ ,$$

$$\lambda_n=\begin{cases}1 & \text{for } n=0,\\ 2 & \text{for } n\neq 0,\end{cases}$$

where $\vec{q}=\vec{k}_i-\vec{k}_f$ is the momentum transfer to the target, $\vec{v}_i$ is the velocity of the incident electron, $\vec{b}$ is the impact parameter vector, J_n's are the Bessel functions, and the angles (θ_m,ϕ_m) define the orientation of the molecular axis $\vec{R}$ with respect to the polar axis which is taken to be the direction of $\vec{k}_i$. When the above expression is used in Eqs. (1) and (2) we get

$$I(J\rightarrow J',\theta)=\frac{k_i^2(2J'+1)}{4}\sum_{M=-J}^{J}\sum_{M'=-J'}^{J'}\left|\left[\frac{(J-|M|)!}{(J+|M|)!}\frac{(J'-|M'|)!}{(J'+|M'|)!}\right]^{1/2}\times\int P_J^{|M|}(\cos\theta_m)f_{2n,n}(\theta,\theta_m)P_{J'}^{|M'|}(\cos\theta_m)\sin\theta_m\,d\theta_m\right|^2\ , \tag{5}$$

and

$$\langle I(\theta)\rangle=\frac{k_i^2}{2}\sum_{n=0}\int\lambda_n f_{2n,n}^2(\theta,\theta_m)\sin\theta_m\,d\theta_m\ , \tag{6}$$

where $2n=|M-M'|$. Total cross section $\sigma(J\rightarrow J')$ for the transition $J\rightarrow J'$ or the average total cross section $\langle\sigma\rangle$ are readily computed using Eq. (5) or Eq. (6) in

$$\sigma=2\pi\int_0^\pi I\sin\theta\,d\theta\ . \tag{7}$$

Average cross sections $\langle I(\theta)\rangle$ and $\langle\sigma\rangle$ include all the possible final rotational states for any initial rotational state J of the target molecule.

III. EFFECTIVE POTENTIAL

We have taken the following form of the electron-molecule interaction:

$$V(\vec{r},\hat{R})=V_s(\vec{r},\hat{R})+V_{\rm ex}(\vec{r},\hat{R})+V_p(\vec{r},\hat{R})\ , \tag{8}$$

where the static potential $V_s(\vec{r},\hat{R})$ is the electrostatic interaction between the scattered electron and the unperturbed ground-electronic-state charge distribution of the molecule, $V_{\text{ex}}(\vec{r},\hat{R})$ is the effective local potential which takes into account the effect of electron exchange, and $V_p(\vec{r},\hat{R})$ is the polarization potential. When the model effective electron-molecule interaction potential given by Eq. (8) is inserted in Eq. (3) the first two coefficients of the Legendre expansions become

$$V^0(r)=V_s^0(r)+V_{\text{ex}}^0(r)+V_p^0(r)\ , \tag{9}$$

$$V^2(r)=V_s^2(r)+V_{\text{ex}}^2(r)+V_p^2(r)\ , \tag{10}$$

with

$$V_p^0(r)=-\frac{\alpha_0}{2r^4}f_c(r,r_c)\ ,$$

$$V_p^2(r)=-\frac{\alpha_2}{2r^4}f_c(r,r_c)\ ,$$

$$f_c(r,r_c)=1-\exp[-(r/r_c)^6]\ ,$$

where α_0 and α_2 are, respectively, the spherical and nonspherical parts of the static dipole polarizability, $f_c(r,r_c)$ is the cutoff function, and r_c is the cutoff parameter. α_0 and α_2 are taken[66] to be equal to $11.9e^2a_0^3$ and $3.13e^2a_0^3$, respectively.

Semiempirical and *ab initio* calculations of $V_s^0(r)$ and $V_s^2(r)$ are available[31,67] for the system e-N_2. However, we have obtained them using the atomic potentials calculated by Cox and Bonham[68] (the equilibrium internuclear separation being taken as $2.068a_0$). To reproduce the quadrupole tail of $V_s^2(r)$ properly we have used

$$V_s^2(r) \underset{r\to\infty}{\sim} -Q/r^3\ ,$$

in which the experimental quadrupole moment[69] $Q=-1.13e^2a_0^2$ has been substituted, the smoothing out having been done by making use of the cutoff function $f_c(r,r_c)$. In Table I the present static potential has been compared with the accurate *ab initio* [432] static potential calculated by Truhlar *et al.*[67]

The cutoff function $f_c(r,r_c)$ is introduced since the small-r form of the long-range potentials, $V_p^0(r)$ and $V_p^2(r)$, is not known accurately. The restriction on $f_c(r,r_c)$ is twofold: it should make these potentials vanish at the center of mass of the two nuclei[70] and, upon a proper choice of the cutoff parameter r_c, it should reproduce the experimental cross sections as accurately as possible. In this paper we have used a form[71] for $f_c(r,r_c)$ similar to one used by us for the hydrogen molecule (model B, Ref. 53) with $r_c=2a_0$. This value of r_c is within the range ($1.3a_0 \lesssim r_c \lesssim 2.1a_0$) suggested by Breig and Lin[72] from an analysis of the structure of N_2. It also lies between the values $2.308a_0$ and $1.592a_0$ determined semiempirically by adjusting calculated low-energy resonance energy, with[9] and without[73] exchange, respectively, to agree with experiment by Burke and co-workers. A similar analysis with exchange, owing to Morrison and Collins,[11] produced a cutoff parameter equal to $2.341a_0$. Since we have not considered exchange, test calculations at 30 eV with $r_c=1.592a_0$ are performed and these will be discussed in Sec. IV.

TABLE I. Legendre coefficients V_s^0 and V_s^2 of the static potential for e-N_2 scattering in Hartree atomic units.

$r\,(a_0)$	V_s^0 Present	V_s^0 *Ab initio*[a]	V_s^2 Present	V_s^2 *Ab initio*[a]
0.0	−2.140	−1.882	0.000	0.000
0.2	−2.184	−1.942	−0.323	−0.324
0.4	−2.314	−2.114	−1.304	−1.311
0.6	−2.525	−2.382	−2.980	−2.998
0.8	−2.810	−2.737	−5.446	−5.490
1.0	−3.277	−3.225	−9.190	−9.157
1.2	−2.171	−2.158	−5.586	−5.630
1.4	−1.327	−1.324	−3.047	−3.095
1.6	−0.816	−0.814	−1.707	−1.744
2.0	−0.307	−0.303	−0.510	−0.547
2.4	−0.116	−0.112	−0.141	−0.160
2.8	−0.045	−0.041	−0.024	−0.035
3.2	−0.017	−0.015	0.004	0.002
4.0	−0.003	−0.002	0.014	0.012
5.0	−0.000	−0.000	0.009	0.008

[a] Potential [432] in Ref. 67. The calculated quadrupole moment $Q=-0.9923e^2a_0^2$.

The effect of electron exchange in scattering processes is important at low energies and a number of models[11,15,74,75] for local exchange potentials $V_{\text{ex}}^0(r)$ and $V_{\text{ex}}^2(r)$ are in use. In the present study we have neglected the effect of exchange which is not very important[76] for the e-N_2 scattering in the energy region considered here.

Finally, we like to point out that the maximum number of terms $\nu_{\max}$ as high as 28 is often required[11,35] in the one-center expansion (3) to represent accurately the e-N_2 potential, and in the close-coupling calculation cross sections are usually made to converge[11,26] with respect to increasing $\nu_{\max}$. Thus, the truncation of the expansion (3) at $\nu_{\max}=2$ is rather a very simple approximation for a complex molecule like nitrogen, but we cannot take more than two terms in the present formulation.

IV. RESULTS AND DISCUSSIONS

A. Numerical integration and cross sections

To compute the cross sections we need to perform numerically the two-dimensional integration in Eqs. (5) and (6) and the one-dimensional integration in $X(b,\theta_m)$ and $\gamma(b,\theta_m)$. The angular integration within the range $\theta_m=0$ to 90° is performed[77] using eight-point Gauss-Legendre quadrature (unless otherwise specified). For b and z integration the integrated range is divided into a number of meshes, depending upon energy, with variable step sizes and each mesh is then integrated using eight-point Gauss-Legendre quadrature. Total cross sections are computed by using Simpson's rule. Average cross sections are found to converge if only the first three terms in Eq. (6) are taken into consideration.

In the present paper we have calculated differential and total cross sections for two pure elastic processes $(J=0\rightarrow J'=0)$ and $(J=1\rightarrow J'=1)$ and for two rotational-excitation processes $(J=0\rightarrow J'=2)$ and $(J=1\rightarrow J'=3)$ at impact electron energies 20–200 eV. Momentum-transfer cross sections for the above processes are also obtained. Within the same energy interval we have further computed the average elastic differential, total, and momentum-transfer cross sections. In Figs. 1 and 2 the differential-scattering cross sections (DCS) for some of the processes mentioned earlier at and below 50 eV are plotted against the scattering angles. Average elastic DCS $\langle I(\theta)\rangle$ calculated by us are compared with those of other experimental and theoretical workers in the Figs. 3–5. In Table II state-to-state DCS $I(J\rightarrow J',\theta)$ at 30 eV are given. Average elastic differential cross sections at 20–200 eV are given in Table III. Total and momentum-transfer cross sections are presented in Tables IV and V, respectively, along with those obtained experimentally or theoretically by different investigators.

B. Pure elastic and rotational-excitation cross sections

The solid curve in Fig. 1 shows the DCS for the pure elastic process $(J=0\rightarrow J'=0)$ at 30 eV and is representative of those for other energies as well as for the process $(J=1\rightarrow J'=1)$. The general features of $I(0\rightarrow 2,\theta)$ at 20–50 eV and $I(1\rightarrow 3,\theta)$ at 20 and 50 eV are shown in Fig. 2. At a particular scattering angle $I(0-2,\theta)$ is always higher than $I(1-3,\theta)$. The maxima or the minima in DCS for both the processes, however, occur at the same scattering angle. This angle decreases with increasing energy. Around the forward direction the cross sections are found to decrease very sharply (DCS exhibit an oscillatory feature roughly between $0-5^0$ and these are not shown in the figure). The state-to-state cross sections are found to depend upon the initial rotational state J. With the increase in the initial state J, cross sections increase for elastic processes while they decrease for the inelastic processes. These characteristics resembled those observed by us in the case of the hydrogen molecule[53]

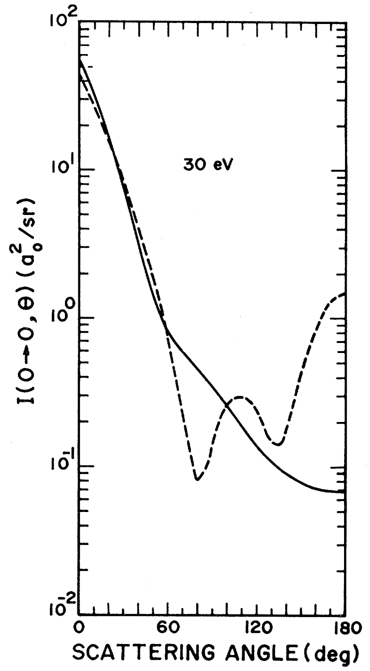

FIG. 1. Pure elastic differential scattering cross sections for the process $J=0\rightarrow J'=0$ at 30 eV as a function of scattering angle. ——, present calculation; - - - - - -, Onda and Truhlar (Ref. 34: potential ix and basis set XX/2–6).

Separation of pure elastic scattering and rotational-excitation cross sections have not yet been obtained experimentally for the nitrogen molecule with the energy resolution achieved so far in the laboratory. With the hydrogen molecule a few measurements[78,79] have been carried out for the rotational-excitation cross sections for the process $(J=1\rightarrow J'=3)$. All these experimental results are for impact electron energies at or below 12 eV excepting those of Srivastava *et al.*[79] who have

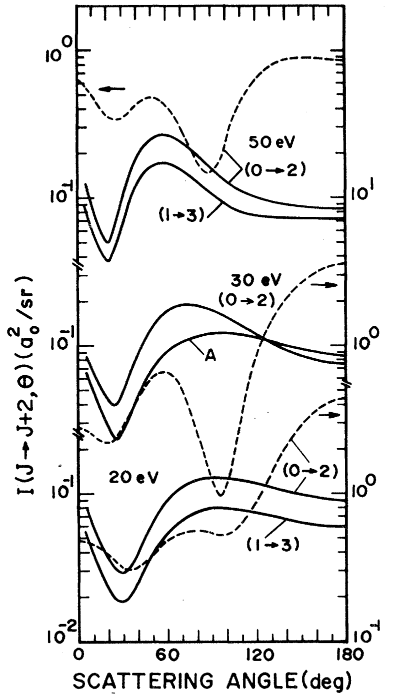

FIG. 2. Rotational-excitation differential scattering cross section for the processes $J=0\to J'=2$ (at 20–50 eV) and $J=1\to J'=3$ (at 20 and 50 eV) as a function of scattering angle. ——, present calculation; curve A, present calculation with $r_c=1.592a_0$; — — — —, at 20 and 30 eV (right-hand-side ordinate), Onda and Truhlar (potential ix and basis set XX/2–6 or XX/2–12, Ref. 34); and at 50 eV, Onda and Truhlar (potential viii and basis set XX/2, Ref. 32). Cross sections of Onda and Truhlar are for the process $J=0\to J'=2$.

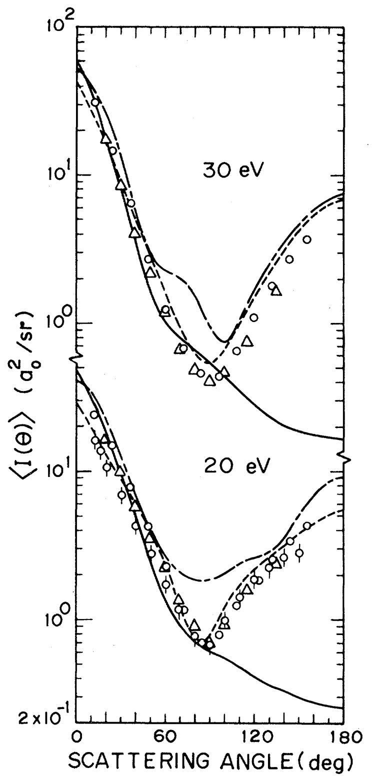

FIG. 3. Average elastic differential scattering cross sections at 20 and 30 eV as a function of scattering angle. Experimental: ○, Shyn and Carignan (Ref. 59); Δ, revised data of Srivastava *et al.* (Ref. 61), see Sec. IV C; ɸ, DuBois and Rudd (Ref. 62). Theoretical: ——, present calculation; —-—, Seigel *et al.* (Ref. 16); — — — —, Onda and Truhlar (potential ix and basis set XX/2–6 or XX/2–12, Ref. 34).

covered the energy region 3–100 eV. Srivastava *et al.* observed that the rotational-excitation cross sections exceed the pure elastic cross sections at large scattering angles. Calculations for the hydrogen molecule,[52,53,80,81] including those with the present method[52,53] confirmed this observation. For the nitrogen molecule, however, this is observed at $E\geq30$ eV for the process $J=0\to J'=2$. Onda and Truhlar[34] obtained similar results even at 20 eV.

The close coupling $I(0\to0,\theta)$ at 30 eV (Ref. 34) and $I(0\to2,\theta)$ at 20–50 eV (Refs. 32 and 34) obtained by Onda and Truhlar are shown in Figs. 1 and 2, respectively, for comparison. The angular shape of $I(0\to2,\theta)$ between the scattering angles 0°–90° is strikingly similar to that of the present one, although the magnitude of the cross sections is about 5 to 10 times higher. The $I(0\to2,\theta)$ at comparable energy obtained by Rahman *et al.*[55] considering only the asymptotic part of the static potential gives a completely different angular dependence (not shown). As is evident from Fig. 2 (curve A, 30 eV) lowering of the cutoff parameter from $2a_0$ to $1.592a_0$ reduces the magnitude of the inelastic cross sections over most of the angular range.

C. Average elastic differential scattering cross sections

In Figs. 3–5 we have presented the average elastic DCS at energies 20–200 eV. Comparison is made with a few recent experimental measurements[59–63] at energies which overlap with those of ours. Very recently Shyn and Carignan[59] have reported normalized measurements at 1.5–400 eV and at –96°–156° replacing the relative measure-

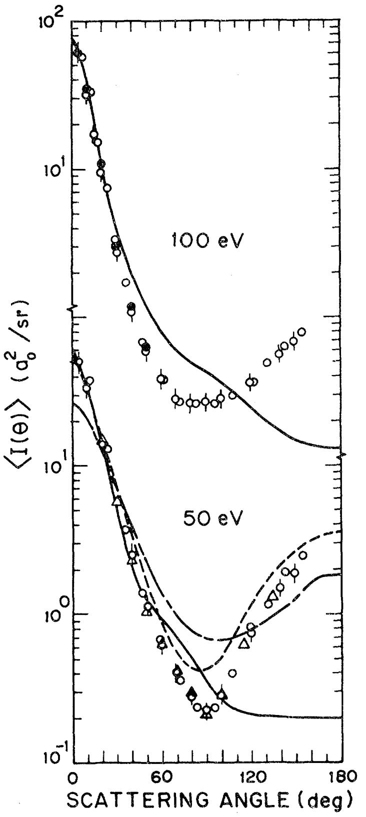

FIG. 4. Average elastic differential-scattering cross sections at 50 and 100 eV as a function of scattering angle. Experimental: ○, Shyn and Carignan (Ref. 59): Δ, revised data of Srivastava *et al.* (Ref. 61), see Sec. IV C; ϕ, DuBois and Rudd (Ref. 62); ●, Jansen *et al.* (Ref. 63). Theoretical: ——, present calculation; — — — —, Onda and Truhlar (potential viii and basis set XX/2, Ref. 32); ‒‒‒, Sawada *et al.* (Ref. 41), tabular values are given in Ref. 31.

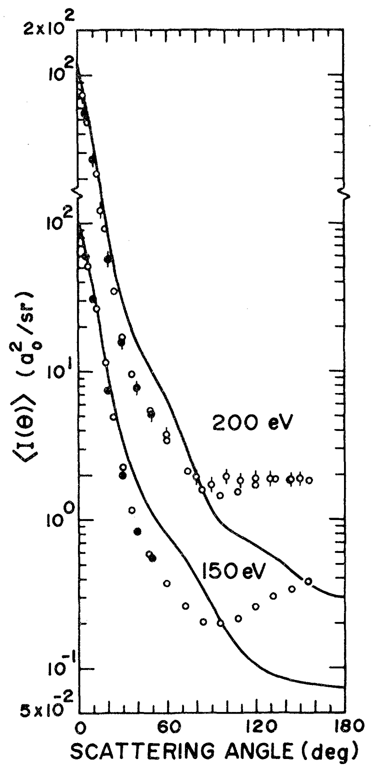

FIG. 5. Average elastic differential scattering cross sections at 150 and 200 eV as a function of scattering angle. Experimental: ○, Shyn and Carignan (Ref. 59); ϕ, DuBois and Rudd (Ref. 62); ●, Jansen *et al.* (Ref. 63). Theoretical: ——, present calculation.

ments of Shyn *et al.*[6] at 5–90 eV and at 3°–160°. Jansen *et al.*[63] reported normalized measurements at 100–3000 eV and at 5°–55°. The measurements of DuBois and Rudd[62] at 20–80 eV and 2°–150° were absolute. Srivastava *et al.*[61] determined the ratios between the average elastic DCS for N_2 and elastic DCS for He and obtained the average elastic DCS for N_2 utilizing the elastic DCS for He measured by McConkey and Preston.[82] Recently, more accurate data[83] for He have been reported from the laboratory of Trajmar and we have used these to recover the absolute average elastic DCS for N_2 for comparison. Measurements of Srivastava *et al.* were for the scattering angles 20°–135° and at energies 5–75 eV.

The striking feature of the experimental DCS is the occurrence of a sharp minimum around the scattering angle 90° at low energies which tends to diminish at higher and higher energies. The present theoretical cross sections fail to reproduce this feature of the experimental cross sections. However, below the scattering angle 90° and up to the smallest angle at which experimental measurements are available, the overall agreement between the theoretical predictions and experimental observations is very good at energies 20–50 eV. At still higher energies the angular region, at which good agreement occurs, tends to contract from the large-angle side. This is exactly in accordance with the type of approximation we have used in the present calculations.

The small-angle measurements of DuBois and Rudd, Jansen *et al.* and Shyn and Carignan at 100–200 eV are in excellent agreement, both in magnitude and shape, with the present calculations. This is also true for the measurements of DuBois and Rudd at 50 eV, and those of Shyn and Carignan, and Srivastava *et al.* at impact energies

TABLE II. State-to-state differential scattering cross sections (in a_0^2/sr) for e-N_2 scattering at 30 eV.

θ (deg)	$I(0\rightarrow0)$	$I(0\rightarrow2)$ $\times10^{-2}$	$I(1\rightarrow1)$	$I(1\rightarrow3)$ $\times10^{-2}$	$I(0\rightarrow0)^a$	$I(0\rightarrow2)^a$ $\times10^{-2}$	$I(1\rightarrow1)^a$	$I(1\rightarrow3)^a$ $\times10^{-2}$
0	56.21		56.23		57.62		57.62	
5	44.25	8.55	44.29	5.24	46.05	6.76	46.08	4.12
10	32.76	6.97	32.79	4.28	34.81	5.28	34.83	3.23
15	23.68	5.41	23.70	3.34	25.77	3.91	25.79	2.40
20	16.67	4.23	16.69	2.61	18.65	2.77	18.66	1.71
25	11.42	3.99	11.44	2.46	13.17	2.33	13.18	1.44
30	7.623	4.81	7.642	2.93	9.076	2.66	9.086	1.63
35	4.985	6.48	5.011	3.93	6.126	3.55	6.140	2.15
40	3.230	8.73	3.265	5.27	4.076	4.75	4.095	2.87
50	1.435	13.6	1.489	8.21	1.823	7.32	1.852	4.41
60	0.805	17.4	0.874	10.5	0.949	9.45	0.986	5.69
70	0.579	19.1	0.655	11.6	0.641	10.9	0.685	6.61
80	0.452	19.1	0.529	11.6	0.518	11.9	0.565	7.21
90	0.346	17.8	0.417	10.9	0.438	12.4	0.487	7.54
100	0.256	15.9	0.320	0.83	0.366	12.4	0.416	7.62
110	0.187	14.0	0.243	8.71	0.300	12.1	0.349	7.46
120	0.139	12.1	0.188	7.68	0.245	11.5	0.291	7.15
130	0.109	10.6	0.151	6.83	0.203	10.8	0.246	6.76
140	0.090	9.41	0.128	6.16	0.310	10.1	0.313	6.38
150	0.079	8.57	0.110	5.70	0.150	9.47	0.188	6.06
160	0.073	8.00	0.105	5.39	0.136	9.00	0.172	5.80
170	0.069	7.69	0.100	5.22	0.128	8.74	0.163	5.66
180	0.068	7.59	0.099	5.17	0.126	8.65	0.161	5.61

[a] With the cutoff parameter $r_c=1.592a_0$ (θ_m integration was performed with four-point Gauss-Legendre quadrature).

20–50 eV. At 20 eV and small scattering angles the present cross sections show a steeper angular dependence in comparison with the results of DuBois and Rudd. So far as the shape of the DCS is concerned, the earlier relative measurements by Shyn *et al.*,[60] when normalized with the present results at 15°, are found to be in better agreement (not shown). Mention may be made here of the relative measurements of Finn and Doering[64] (not plotted) at 13–100 eV and 5°–90°. These measurements at overlapping energies show relatively slower increase at small scattering angles.

We now compare our results with those obtained theoretically by other investigators. A comprehensive theoretical investigation of e-N_2 scattering at the lower part of the intermediate-energy region was carried out by Onda and Truhlar following the effective potential approach.[25] Treating the nitrogen molecule as a rigid rotor they applied[29] the laboratory-frame[39] converged close-coupling approximation to compute the elastic scattering and rotational-excitation cross sections at 30 and 50 eV. In addition to static potential they considered a local exchange potential in the semiclassical approximation (SCE)[25,75] and a semiempirical polarization potential similar to one used in the present paper, but with a cutoff parameter determined by Buckley and Burke.[9] The static and exchange potentials were obtained using semiempirical molecular orbital theory (INDOXI/1s).[25,67] This calculation updated the earlier unconverged close-coupling calculation of Brandt *et al.*[27] A similar calculation but with a self-consistent-field adiabatic polarization potential[84] without containing any adjustable parameter were performed[30] at 30 eV. The electron-molecule potential was further improved[31] to incorporate more accurately the quadrupole interaction in the static potential, the effect of polarization on the exchange term (SCE), and the r^{-6} term in the long-range polarization interaction. The computation was done at 50 eV using the earlier method, but with a channel decoupling procedure (centrifugal dominant approximation) which simplifies the calculation considerably. Then the vibrational motion was allowed[32,34] and treated by the vibrational sudden approximation; still treating the rotational motion by the earlier method, calculations were performed at 10–50 eV. In these cal-

TABLE III. Average elastic differential scattering cross sections, $\langle I(\theta)\rangle$, for e-N_2 scattering (in a_0^2/sr).

E(eV) θ(deg)	20	30	30[a]	50	100	150	200
0	48.11	56.28	57.64	66.03	84.06	102.4	117.7
5	39.45	44.35	46.12	48.74	56.26	64.41	70.13
10	30.59	32.85	34.87	33.36	34.11	36.00	36.23
15	23.36	23.74	25.82	21.89	19.38	18.64	17.13
20	17.54	16.72	18.68	13.76	10.59	9.478	8.161
25	12.95	11.47	13.20	8.321	5.912	5.233	4.448
30	9.394	7.683	9.110	4.949	3.662	3.339	2.865
35	6.715	5.062	6.168	3.016	2.598	2.374	2.042
40	4.750	3.329	4.131	1.995	2.009	1.769	1.537
50	2.383	1.583	1.904	1.238	1.249	1.077	0.985
60	1.314	0.990	1.051	0.963	0.789	0.776	0.648
70	0.882	0.782	0.759	0.720	0.587	0.586	0.378
80	0.708	0.657	0.646	0.503	0.507	0.411	0.203
90	0.616	0.539	0.572	0.352	0.446	0.270	0.119
100	0.544	0.431	0.502	0.268	0.377	0.178	0.089
110	0.476	0.344	0.435	0.228	0.308	0.128	0.077
120	0.414	0.279	0.375	0.213	0.249	0.103	0.069
130	0.362	0.235	0.326	0.207	0.205	0.091	0.059
140	0.320	0.205	0.289	0.205	0.173	0.085	0.049
150	0.290	0.187	0.263	0.203	0.153	0.082	0.041
160	0.269	0.176	0.245	0.202	0.140	0.077	0.035
170	0.258	0.170	0.235	0.201	0.133	0.075	0.031
180	0.254	0.168	0.232	0.201	0.131	0.074	0.030

[a] With the cutoff parameter $r_c = 1.592a_0$ (θ_m integration was performed with four-point Gauss-Legendre quadrature).

culations, except at 50 eV,[32] the local exchange potential was approximated[32,34] using the Hara-free-electron-gas exchange approximation (HFEGE)[74] which is found[11,33,34,37] to be more accurate at lower energies and at large scattering angles. Sawada *et al.*[41] considered an independent-particle model with a regularization factor and quadrupole and semiempirical polarization potentials with a cutoff parameter $r_c = 2a_0$. They used the fixed nuclei approximation to calculate average elastic differential and total cross sections at impact energies 10—500 eV. Wedde and Strand[42] used the independent-atom approximation and made partial-wave calculations for the energy interval 40—1000 eV, polarization and exchange effects were not included. Dill and Dehmer[15] used the continuum-multiple-scattering method and Slater exchange approximation in the frame work of fixed-nuclei theory to calculate the elastic total scattering cross sections for 0—1000 eV, but the average elastic DCS were reported only at energies between 0—30 eV by Siegel *et al.*[16] In a recent computation[17] they have considered exchange using HFEGE and SCE approximations. A two-potential approach, similar to the polarized orbital method, in which the long-range interactions are treated using the Born approximation was used by Choi *et al.*[43] They calculated the average elastic differential and total cross sections at 50—500 eV in addition to the vibrational excitation cross sections.

In Figs. 3 and 4 comparison is made with the converged close-coupling $\langle I(\theta)\rangle$ at 20—50 eV obtained by Onda and Truhlar.[32,34] We have also displayed those theoretical $\langle I(\theta)\rangle$ for which tabular values are available, namely, at 20 and 30 eV due to Siegel *et al.*[16] and at 50 eV due to Sawada *et al.*[31,34] The close-coupling calculations give the best fit to the measurements at almost all scattering angles. The overall agreement of the present calculations with the predictions of the close-coupling approximation is fairly satisfactory between the scattering angles 0°—90°. At small scattering angles, the best agreement is found for 50 eV impact energy. At 20 and 30 eV the present cross sections show a steeper rise, but they are in better agreement with the experimental observa-

TABLE IV. Total cross sections (in a_0^2) for e-N_2 scattering.

Energy (eV)	$\sigma(0\rightarrow0)$	$\sigma(0\rightarrow2)$	$\sigma(1\rightarrow1)$	$\sigma(1\rightarrow3)$	$\langle\sigma\rangle$	$\langle\sigma\rangle^a$
20	28.23	1.27	28.74	0.78	29.61	43.21[b]
	26.9[h]	12.0[h]			41.9[h]	40.8[c]
					46.0[j]	32.60[d]
					69.27[l]	40.00[f]
30	24.14	1.68	24.81	1.04	26.02	36.78[b]
	27.93[g]	1.23[g]	28.43[g]	0.76[g]	29.31[g]	33.2[c]
	23.9[h]	10.2[h]			39.3[h]	31.43[f]
					42.4[j]	
		0.79[m]				
50	19.08	1.93	19.86	1.33	21.61	30.35[b]
	19.4[i]	5.81[i]			31.1[i]	26.0[c]
					25.0[j]	25.8[d]
					27.5[k]	20.35[f]
					27.3[l]	
					37.4[n]	
100	15.58	3.35	16.92	2.46	20.10	20.00[b]
					22.5[n]	17.70[d]
						18.50[e]
						13.57[f]
150	14.11	3.57	15.54	2.58	18.75	16.07[b]
200	12.80	3.44	14.17	2.40	17.03	13.21[b]
					14.8[n]	12.6[d]
						13.2[e]

[a] Experimental.
[b] Reference 59.
[c] Reference 61 (reanalyzed by Onda and Truhlar, Refs. 32 and 34).
[d] Reference 62.
[e] Reference 63 (as reported in Ref. 62).
[f] Reference 64.
[g] Present calculation with the cutoff parameter $r_c = 1.592a_0$.
[h] Reference 34 (potential ix and basis set XX/2—6 or XX/2—12).
[i] Reference 32 (potential viii and basis set XX/2).
[j] Reference 17 (for 20 and 30 eV as reported in Ref. 34). For 50 eV, Ref. 15 (model B).
[k] Reference 41 (reported in Ref. 32).
[l] Polarized Born (model a), 20 eV (Truhlar *et al.*, Ref. 23) and 50 eV, Ref. 32.
[m] Reference 55 (extrapolated value).
[n] Reference 43.

tions. The present approximation is superior to one used by Siegel *et al.*[16] or by Sawada *et al.* in predicting the small-scattering-angle cross sections.

The polarization potential is somewhat energy dependent. Jansen *et al.*[63] obtained an apparent polarizability for N_2 from their measured cross sections at different energies. They found that the apparent polarizability depends considerably on energy. It equals the static polarizability only at very high energy and increases significantly from the static polarizability as one goes towards lower energies. The increase is as much as 50% at 100 eV, the lowest energy of their measurements. As such, the same value of the cutoff parameter r_c would not be, in general, appropriate for the description of the scattering processes involving low- to intermediate-energy electrons. We have not considered this dependence of cross sections on r_c. However, we have computed, as a test case, differential cross sections at 30 eV with $r_c = 1.592a_0$ obtained empirically from a low-energy theoretical calculation[73] neglecting the effect of electron exchange, and these are included in Tables II—IV for comparison.

TABLE V. Momentum-transfer cross sections (in a^{0^2}) for e-N_2 scattering.

Energy (eV)	$\sigma_m(0\rightarrow0)$	$\sigma_m(0\rightarrow2)$	$\sigma_m(1\rightarrow1)$	$\sigma_m(1\rightarrow3)$	$\langle\sigma_m\rangle$	$\langle\sigma_m\rangle^a$
20	7.11	1.41	7.67	0.87	8.64	29.63^b
	10.3^e	16.1^e			30.9^e	26.4^c
					32.6^g	
30	4.76	1.65	5.41	1.03	6.63	21.43^b
	6.26^d	1.35^d	6.80^d	0.84^d	7.79^d	18.2^c
	6.24^e	14.4^e			27.4^e	
					27.9^g	
					3.95^i	
50	2.87	1.65	3.53	1.19	5.19	14.64^b
	2.73^f	6.90^f			18.4^f	12.8^c
					22.9^h	
100	1.62	2.27	2.53	1.84	5.09	6.29^b
					9.64^h	
150	0.92	1.64	1.57	1.41	3.55	4.18^b
200	0.61	1.24	1.11	1.01	2.46	2.68^b
					4.05^h	

[a] Experimental.
[b] Reference 59.
[c] Reference 61 (reanalyzed by Onda and Truhlar, Refs. 32 and 34).
[d] Present calculations with the cutoff parameter $r_c = 1.592a_0$.
[e] Reference 34 (potential ix and basis set XX/2−6 or XX/2−12).
[f] Reference 32 (potential viii and basis set XX/2).
[g] Reference 17 (reported in Ref. 34).
[h] Reference 43.
[i] Reference 57.

D. Total and momentum-transfer cross sections

Total cross sections for different pure elastic and inelastic processes computed using Eqs. (5) and (7) and average total cross sections calculated using Eqs. (6) and (7) at energies 20−200 eV are given in Table IV. For the sake of comparison the average total cross sections measured[59,61−64] by and obtained theoretically[15,17,23,32,34,41,43,55] by different workers are also included in the table. As is evident from the table, the experimental average elastic total cross sections obtained by different workers are in very good agreement with our theoretical cross sections. The best agreement occurs with the measurements of DuBois and Rudd[62] which are within 10% at energies 20−100 eV. At 20−50 eV the present cross sections are about 30% lower than the converged close-coupling cross sections of Onda and Truhlar.[32,34] This is quite encouraging in view of the simple electron-molecule potential, which does not contain even the effect of electron exchange, used in the present study. The discrepancy is maximum with the calculation of Siegel *et al.*[17] at 20 and 30 eV, apart from the polarized Born calculations at 20 eV by Truhlar *et al.*[23] A comparative close-coupling study by Rumble and Truhlar[36] resulted in an increase of 30% in the total scattering cross section at and below 30 eV when the potential is constrained by the assumptions of the multiple scattering method of Siegel *et al.*[17] The agreement with the other theoretical calculations is fairly good throughout the energy interval considered here.

The state-to-state total cross section depends upon the initial rotational state J of the molecule; the pure elastic cross sections increases while the inelastic cross section decreases with increasing J. No previous calculations are available for which the initial state is $J=1$. At 20−50 eV and for $J=0$, the pure elastic cross sections $\sigma(0\rightarrow0)$ are comparable with those obtained by Onda and Truhlar,[32,34] while the contribution to the average total cross sections $\langle\sigma\rangle$ due to the rotational excitation of the molecule is very much smaller. For example, the sum total of rotational-excitation cross sections is about eight times too small at 30 eV. This indicates the importance of the inclusion of terms greater than $\nu=2$ in the one-center expansion of the electron-molecule potential. Since the major contribution to rotational-excitation cross sections comes through the process $J=0\rightarrow J'=2$ which is dominated by the term $\nu=2$, an accurate evaluation of this term is essential. At 30 eV, the cross section $\sigma(0\rightarrow 2)$ is six times lower than that obtained by Onda and Truhlar,[34] but substantial improvement is achieved over the calculation of Rahman *et al.*[55]

In Table V various momentum-transfer cross sections at 20–200 eV are presented. The experimental cross sections of Shyn and Carignan[59] at 20–200 eV, Srivastava *et al.*[32,34,61] at 20–50 eV, and the theoretical cross sections of Onda and Truhlar,[32,34] Siegel *et al.*,[17] Choi *et al.*,[43] and Gianturco *et al.*[56] at relevant energies are also shown for comparison. The agreement is very poor at 20–50 eV, but reasonably good at 100–200 eV. This is not surprising since the present method is inadequate for representing the large-angle scattering.

IV. CONCLUSIONS

We would like to point out two inherent limitations of the present investigation. First, the Glauber-type eikonal amplitude is not valid for large-angle scattering. Second, in the single-center expansion of the electron-molecule potential Eq. (3) we have considered only the first two nonvanishing terms; this is not adequate for representing a complex molecule like nitrogen. The inclusion of higher-order terms would make the expressions for cross sections complicated and the computation difficult. Even with the last mentioned limitation we find that the Glauber-type eikonal amplitude predicts average elastic cross sections, both differential and total, which are close to those observed experimentally by different workers. The angular shape and magnitude of the experimental average elastic cross sections are well reproduced over a considerable range of scattering angles, particularly at small scattering angles, throughout the energy region considered here. The qualitative features of the rotational-excitation cross sections resemble those obtained by the close-coupling approximation. A more realistic potential such as the potential viii or ix of Onda and Truhlar,[32,34] even if it is truncated at $\nu=2$, might have given better agreement with the experimental results and with the predictions of the sophisticated close-coupling approximation. In summary, the Glauber-type eikonal approximation, which is a mathematically and computationally simple approach, yields reasonably good estimates of the electron-molecule elastic scattering and rotational-excitation cross sections. Hence, this approximation might be considered to be an effective tool for studying complex molecular targets for which close-coupling calculations are prohibitively difficult.

ACKNOWLEDGMENT

The authors are grateful to Professor D. G. Truhlar, University of Minnesota, for sending the tabular data computed by his group and to Dr. A. S. Ghosh, Indian Association for the Cultivation of Science, Calcutta-700032, for helpful discussions. This work was supported by the Indian Space Research Organization under Project No. 10/2(1)/76-III.

---

[1] H. C. Stier, Z. Phys. 76, 439 (1932).
[2] J. B. Fisk, Phys. Rev. 49, 167 (1936).
[3] E. Gerjuoy and S. Stein, Phys. Rev. 97, 1671 (1955).
[4] Yu. D. Oksyuk, Zh. Eksp. Teor. Fiz. 49, 1261 (1965) [Sov. Phys.—JETP 22, 873 (1966)].
[5] K. Takayanagi and S. Geltman, Phys. Rev. 138, A1003 (1965).
[6] D. H. Sampson and R. C. Mjolsness, Phys. Rev. 140, A1466 (1965).
[7] S. Geltman and K. Takayanagi, Phys. Rev. 143, 25 (1966).
[8] P. G. Burke and A. L. Sinfailam, J. Phys. B 3, 641 (1970).
[9] B. D. Buckley and P. G. Burke, J. Phys. B 10, 725 (1977).
[10] M. A. Morrison and L. A. Collins, J. Phys. B 10, L119 (1977).
[11] M. A. Morrison and L. A. Collins, Phys. Rev. A 17, 918 (1978).
[12] M. A. Morrison and B. I. Schneider, Phys. Rev. A 16, 1003 (1977).
[13] C. W. McCardy, Jr., T. N. Rescigno, and V. McKoy, J. Phys. B 9, 691 (1976).
[14] N. Chandra and A. Temkin, Phys. Rev. A 13, 188 (1976); 14, 507 (1976).
[15] D. Dill and J. L. Dehmer, Phys. Rev. A 16, 1423

(1977).

[16] J. Siegel, D. Dill, and J. L. Dehmer, Phys. Rev. A 17, 2106 (1978).

[17] J. Siegel, J. L. Dehmer, and D. Dill, Phys. Rev. A 21, 85 (1980).

[18] J. D. Craggs and H. S. W. Massey, in *Handbuch der Physik,* edited by J. D. Craggs and H. S. W. Massey (Springer, Berlin, 1959), Vol. 37, p. 314.

[19] K. Takayanagi and Y. Itikawa, in *Advances in Atomic and Molecular Physics,* edited by D. R. Bates and I. Esterman (Academic, New York, 1970), Vol. 6, p. 105.

[20] D. E. Golden, N. F. Lane, A. Temkin, and E. Gerjuoy, Rev. Mod. Phys. 43, 642 (1971).

[21] N. F. Lane, Rev. Mod. Phys. 52, 1 (1980), and references therein.

[22] D. G. Truhlar and J. K. Rice, J. Chem. Phys. 52, 4480 (1970); 55, 2005(*E*) (1971).

[23] D. G. Truhlar, S. Trajmar, and W. Williams, J. Chem. Phys. 57, 3250 (1972); D. G. Truhlar, *ibid.* 57, 3260 (1972). See also Ref. 32 below.

[24] A. C. Yates and A. Tenny, Phys. Rev. A 5, 2474 (1972).

[25] D. G. Truhlar, in *Semiempirical Methods of Electronic Structure Theory, Part B: Application,* edited by G. A. Segal (Plenum, New York, 1977), p. 247.

[26] D. G. Truhlar, K. Onda, R. A. Eades, and D. A. Dixon, Int. J. Quantum Chem. Symp. 13, 601 (1979).

[27] M. A. Brandt, D. G. Truhlar, and F. A. Van-Catledge, J. Chem. Phys. 64, 4957 (1976).

[28] N. A. Mullaney and D. G. Truhlar, Chem. Phys. Lett. 58, 512 (1978).

[29] K. Onda and D. G. Truhlar, J. Chem. Phys. 69, 1361 (1978).

[30] K. Onda and D. G. Truhlar, J. Chem. Phys. 70, 1681 (1979).

[31] K. Onda and D. G. Truhlar, J. Chem. Phys. 71, 5097 (1979).

[32] K. Onda and D. G. Truhlar, J. Chem. Phys. 71, 5107 (1979).

[33] K. Onda and D. G. Truhlar, J. Chem. Phys. 72, 1415 (1980).

[34] K. Onda and D. G. Truhlar, J. Chem. Phys. 72, 5249 (1980).

[35] J. R. Rumble and D. G. Truhlar, J. Chem. Phys. 70, 4101 (1979); 72, 3441(E) (1980).

[36] J. R. Rumble and D. G. Truhlar, J. Chem. Phys. 72, 3206 (1980).

[37] J. R. Rumble and D. G. Truhlar, J. Chem. Phys. 72, 5223 (1980).

[38] J. R. Rumble, D. G. Truhlar, and M. A. Morrison, J. Phys. B 14, L301 (1981).

[39] A. M. Arthurs and A. Dalgarno, Proc. R. Soc. London Ser. A 256, 540 (1960).

[40] J. L. Dehmer and D. Dill, in *Electron-Molecule and Phonon-Molecule Collisions,* edited by T. Rescigno, V. McKoy, and B. Schneider (Plenum, New York, 1979), p. 225.

[41] T. Sawada, P. S. Ganas, and A. E. S. Green, Phys. Rev. A 9, 1130 (1974).

[42] T. Wedde and T. G. Strand, J. Phys. B 7, 1091 (1974).

[43] B. H. Choi, R. T. Poe, J. C. Sun, and Y. Shan, Phys. Rev. A 19, 116 (1979).

[44] R. G. Glauber, in *Lectures in Theoretical Physics, Summer Institute for Theoretical Physics, University of Colorodo, Boulder, 1958,* edited by W. E. Brittin and L. G. Dunhum (Interscience, New York, 1959), Vol. 1, p. 315.

[45] C. J. Joachain and C. Quigg, Rev. Mod. Phys. 46, 279 (1974), and references therein; J. Callaway, Adv. Phys. 29, 771 (1980), and references therein.

[46] A good many references of the application of the eikonal approximation and its different versions to problems in atomic physics have been cited by W. Williamson, Jr. and G. Foster, Phys. Rev. A 11, 1472 (1975). See also, G. Foster and W. Williamson, Jr., Phys. Rev. A 13, 2023 (1976); J. Phys. B 10, 3129 (1977).

[47] R. N. Madan, Phys. Rev. A 11, 1968 (1975); 12, 2631 (1975).

[48] B. K. Thomas and V. Fanco, Phys. Rev. A 13, 2004 (1976); V. Fanco and A. M. Halpern, *ibid.* 21, 1118 (1980).

[49] V. Fanco, Phys. Rev. A 8, 2927 (1973).

[50] T. N. Chang, R. T. Poe, and P. Roy, Phys. Rev. Lett. 31, 1097 (1973).

[51] P. K. Bhattacharyya and A. S. Ghosh, Phys. Rev. A 12, 480 (1975).

[52] P. K. Bhattacharyya and A. S. Ghosh, Phys. Rev. A 14, 1587 (1976).

[53] P. K. Bhattacharyya, K. K. Goswami, and A. S. Ghosh, Phys. Rev. A 18, 1865 (1978).

[54] O. Ashihara, I. Shimamura, and K. Takayanagi, J. Phys. Soc. Jpn. 38, 1732 (1975).

[55] N. K. Rahman, F. A. Gianturco, and U. T. Lamanna, Phys. Rev. A 18, 74 (1978).

[56] F. A. Gianturco, U. T. Lamanna, and N. K. Rahman, J. Chem. Phys. 68, 5538 (1978).

[57] F. A. Gianturco, U. T. Lamanna, and S. Salvini, Int. J. Quantum Chem. Symp. 13, 579 (1979).

[58] Other than H_2 and N_2 mention may be made of, for example, CO_2 [D. Thirumalai, K. Onda, and D. G. Truhlar, J. Chem. Phys. 74, 6792 (1981), and references therein] and CO [K. Onda and D. G. Truhlar, J. Chem. Phys. 73, 2688 (1980), and references therein].

[59] T. W. Shyn and G. R. Carignan, Phys. Rev. A 22, 923 (1980).

[60] T. W. Shyn, R. S. Stolarski, and G. R. Carignan, Phys. Rev. A 6, 1002 (1972).

[61] S. K. Srivastava, A. Chutjian, and S. Trajmar, J. Chem. Phys. 64, 1340 (1976).

[62] R. D. DuBois and M. E. Rudd, J. Phys. B 9, 2657 (1976).

[63] R. H. J. Jansen, F. J. de Heer, H. J. Luyken, B. van Wingerden, and H. J. Blaauw, J. Phys. B 9, 185

(1976).

[64] T. G. Finn and J. P. Doering, J. Chem. Phys. 63, 4399 (1975).

[65] Atomic units are used throughout this paper.

[66] N. J. Bridge and A. D. Buckingham, Proc. R. Soc. London Ser. A 295, 334 (1966).

[67] D. G. Truhlar, F. A. Van-Catledge, and T. H. Dunning, J. Chem. Phys. 57, 4788 (1972); 69, 2941(*E*) (1978).

[68] M. L. Cox, Jr. and R. A. Bonham, J. Chem. Phys. 47, 2599 (1967).

[69] D. E. Stogryn and A. P. Stogryn, Mol. Phys. 11, 371 (1966).

[70] Lane has suggested that the cutoff function should make $V_p(\vec{r},\hat{R})$ vanish at the nuclei rather than at the gravity center of the molecule. See N. F. Lane, in *Fundamental Interactions in Physcis,* edited by B. Kursunoglu and A. Perlmutter (Plenum, New York, 1973), Vol. 2, p. 297.

[71] For a good discussion of the polarization potential, cutoff function, and cutoff parameter see Refs. 26, 29, and 31.

[72] E. L. Breig and C. C. Lin, J. Chem. Phys. 43, 3839 (1965).

[73] P. G. Burke and N. Chandra, J. Phys. B 5, 1696 (1972).

[74] S. Hara, J. Phys. Soc. Jpn. 22, 710 (1967).

[75] M. E. Riley and D. G. Truhlar, J. Chem. Phys. 63, 2182 (1975); 65, 792 (1976); D. G. Truhlar and N. A. Mullaney, *ibid.* 68, 1574 (1978).

[76] Onda and Truhlar has observed an increase of 15%, due to exchange, in the average elastic total cross section at 30 eV; see Ref. 29. For a comparative study of different models see Refs. 33 and 37.

[77] Burroughs B6700 computer system is used for all computations.

[78] H. Ehrhardt and F. Linder, Phys. Rev. Lett. 21, 419 (1968); F. Linder and H. Schmidt, Z. Naturforsch, A26, 1603 (1971); G. Joyez, J. Comer, and F. H. Read, J. Phys. B 6, 2427 (1973).

[79] S. K. Srivastava, R. I. Hall, S. Trajmar, and A. Chutjian, Phys. Rev. A 12, 1399 (1975).

[80] D. G. Truhlar, R. E. Poling, and M. A. Brandt, J. Chem. Phys. 64, 826 (1976).

[81] D. G. Truhlar and M. A. Brandt, J. Chem. Phys. 65, 3092 (1976).

[82] J. W. McConkey and J. A. Preston, J. Phys. B 8, 63 (1975).

[83] D. Register, S. Trajmar, and S. K. Srivastava, Phys. Rev. A 21, 1134 (1980).

[84] D. G. Truhlar and F. A. Van-Catledge, J. Chem. Phys. 69, 3575 (1978).